

Low power on large scales in just enough inflation models

Erandy Ramirez*

Excellence Cluster Universe, Technische Universität München, Boltzmannstr. 2, 85748 Garching, Germany.

(Dated: April 25, 2022)

An early stage of kinetic energy domination for inflation is applied to single-field quadratic and hybrid-type potentials considering only the amount of inflation necessary to solve the problems of the standard cosmological scenario. Using initial conditions inside the 1-sigma interval of the best-fit cosmological parameters for the potentials, low values for the quadrupole component can be obtained.

PACS numbers: 98.80.Cq

I. INTRODUCTION

Following previous works in which a modification of the chaotic inflation scenario [1] is proposed to quantify the predictions of the $\lambda\phi^4$ potential [2], in this work the idea is further applied to the $m^2\phi^2$ potential and a hybrid inflation potential during the stage when there is effectively a single field leading the dynamics. The intention is to evaluate what the effects of this scenario on different types of potentials are. The implementation of this idea in both cases gives predictions for the inflationary parameters inside the constraints imposed by observations [3]. As previously reported in [4] where specific cutoffs of the primordial spectra are used, an early stage of kinetic energy domination with only an amount of inflation necessary to solve the problems of the standard cosmological scenario naturally gives rise to lower values of the first multipoles of the Cosmic Microwave Background (CMB), this is also studied in [5]. By doing a mode integration to find the best-fit values of this scenario for both potentials, initial conditions inside the 1-sigma interval for the quantities that define this scenario of inflation can match the low value of the quadrupole although at a pivot scale two orders of magnitude bigger than 0.002 Mpc^{-1} . Evaluation at scales closer to 0.05 Mpc^{-1} can also produce lower values of the quadrupole.

Additionally, an initial condition for the perturbations consistent with an early stage of kinetic energy domination is considered. The predictions and results for this case are in accordance to those found in [6], applied to the scenario already mentioned in [4], in which the form of the power spectrum does not show a significant dependence on the choice of initial conditions. In the cases studied here, no previous stage of radiation domination is considered to set the initial conditions for the perturbations or the background evolution [7], [8].

II. NOTATION AND PROCEDURE

This is a complementary work to [2] and follows the same notation and procedure. This scenario considers the existence of an upper bound for the validity of a theory in terms of an effective potential, setting therefore a limit to the total amount of inflation that can be produced. For the application of this scenario, a mode integration for the equations of inflationary perturbations has to be done to find the behavior of the primordial power spectra during the initial stage of kinetic energy domination. This early phase breaks slow-roll dynamics and a power-law parameterization for the spectra cannot be applied. From the mode integration one can use the resulting power spectra to obtain the values of the expansion in multipoles of the CMB anisotropies and the best-fit parameters for a specific potential.

The integration of the equations of motion for the background and perturbations is done with respect to the number of e -foldings N , assuming homogeneity and isotropy from the beginning of inflation:

$$\begin{aligned} \frac{dH}{dN} &= \frac{V}{M_P^2 H} - 3H \\ \frac{d\phi}{dN} &= -\sqrt{6M_P^2 - \frac{2V}{H^2}}. \end{aligned} \quad (1)$$

H is the Hubble rate of expansion, V the potential energy and ϕ the scalar field driving inflation. The conventions followed here are $\dot{\phi} < 0 \Rightarrow H' > 0$ and $H \equiv dN/dt$, where t is cosmic time, therefore $dN > 0$ as $dt > 0$. M_P is the reduced Planck mass defined as $M_P \equiv \frac{m_{\text{pl}}}{8\pi}$ and $m_{\text{pl}} = 1.22 \times 10^{19} \text{ GeV}$ is the Planck mass. The notation is in units where $c = 1, h = 1$.

The equations of scalar and tensor perturbations are [9]

$$\begin{aligned} \frac{d^2 u_k^S}{dN^2} + (1 - \epsilon_1) \frac{du_k^S}{dN} + \left[\left(\frac{k}{aH} \right)^2 - f_S(\epsilon_1, \epsilon_2, \epsilon_3) \right] u_k^S &= 0, \\ \frac{d^2 u_k^T}{dN^2} + (1 - \epsilon_1) \frac{du_k^T}{dN} + \left[\left(\frac{k}{aH} \right)^2 - f_T(\epsilon_1) \right] u_k^T &= 0 \end{aligned} \quad (2)$$

where $f_S(\epsilon_1, \epsilon_2, \epsilon_3) = 2 - \epsilon_1 + \frac{3}{2}\epsilon_2 - \frac{1}{2}\epsilon_1\epsilon_2 + \frac{1}{2}\epsilon_2\epsilon_3 + \frac{1}{4}\epsilon_2^2$ and $f_T(\epsilon_1) = 2 - \epsilon_1$, in terms of the horizon flow functions defined as [10]

$$\epsilon_0 \equiv \frac{H_i}{H}, \quad \epsilon_{m+1} \equiv \frac{1}{\epsilon_m} \frac{d\epsilon_m}{dN}, \quad m \geq 0. \quad (3)$$

* erandy@tum.de

$u_k^{S,T}$ represents the usual gauge-invariant combination of metric and field perturbations for scalar and tensor fluctuations [9], k is the comoving wave number of each perturbation mode.

Following the procedure mentioned in [2], this scenario is applied here to two single-field inflation potentials :

$$V = \frac{1}{2}m^2\phi^2, \quad V = V_0 \left(1 + \frac{\phi^2}{16\pi M_P^2}\right) \quad (4)$$

where the second one corresponds to the hybrid inflation potential in the notation of [11] for the stage where there is effectively one scalar field influencing the dynamics, assuming inflation finishes instantaneously. The conditions under which this happens are studied in [12]. In this case, as there is no natural end of inflation, the value $\phi = 16.3M_P$ is used to stop the process of inflation.

To set the initial values for the perturbations, first Bunch–Davies vacuum initial conditions are considered: scalars:

$$u_k^S = \frac{1}{\sqrt{2k}}e^{-ik\tau_i}, \quad \frac{du_k^S}{dN} = -iu_k^S \left(\frac{k}{a_i H_i}\right), \quad (5)$$

tensors:

$$u_k^T = \frac{1}{\sqrt{k}}e^{-ik\tau_i}, \quad \frac{du_k^T}{dN} = -iu_k^T \left(\frac{k}{a_i H_i}\right). \quad (6)$$

And an initial condition consistent with the solution of kinetic energy domination for the mode equation is also considered [4], [6]:

$$u_k^{S,T}(\tau) = \sqrt{\frac{\pi}{8h_i}}(1 + 2h_i\tau)H_0^{(2)}(k\tau) \quad (7)$$

where τ is conformal time defined as $d\tau = dt/a(t)$, $h = a_{,\tau}/a = aH$, a the scale factor and $H_0^{(2)}$ is a Hankel function defined as $H_n^{(2)}(k\tau) \equiv J_n(k\tau) - iY_n(k\tau)$, with J_n and Y_n Bessel functions and n a positive integer. From this expression, the initial conditions for the scalar and tensor perturbations considering kinetic energy domination in terms of the number of e -foldings are

scalars:

$$u_k^S = \sqrt{\frac{\pi}{8a_i H_i}}H_0^{(2)}\left(\frac{k}{2a_i H_i}\right), \quad (8)$$

$$\frac{du_k^S}{dN} = \sqrt{\frac{\pi}{8a_i H_i}}\left[H_0^{(2)}\left(\frac{k}{2a_i H_i}\right) - \frac{k}{a_i H_i}H_1^{(2)}\left(\frac{k}{2a_i H_i}\right)\right],$$

tensors:

$$u_k^T = \sqrt{\frac{\pi}{4a_i H_i}}H_0^{(2)}\left(\frac{k}{2a_i H_i}\right), \quad (9)$$

$$\frac{du_k^T}{dN} = \sqrt{\frac{\pi}{4a_i H_i}}\left[H_0^{(2)}\left(\frac{k}{2a_i H_i}\right) - \frac{k}{a_i H_i}H_1^{(2)}\left(\frac{k}{2a_i H_i}\right)\right].$$

The expressions for the power spectra are [11]

$$P_R = \frac{k^3}{4\pi^2 M_P^2} \left| \frac{u_k^S}{z_S} \right|^2, \quad P_T = \frac{2k^3}{\pi^2 M_P^2} \left| \frac{u_k^T}{z_T} \right|^2 \quad (10)$$

with $z_S = a\sqrt{\epsilon_1}$, $z_T = a$. The scale factor is normalized to 1 at the beginning of inflation.

In order to obtain the predictions of this scenario, the quantities used to set the initial conditions for the background are the scalar field and the function ϵ_1 . Since this scenario is a modification of chaotic inflation, the initial condition for the scalar field is assumed to be above the Planck scale, at a value that assures to produce only the amount of inflation necessary to solve the problems of the standard cosmological scenario. The initial value of the function ϵ_1 sets the phase of kinetic energy domination from which the system of equations rapidly joins the slow-roll attractor regime. Consequently, the potential is many orders of magnitude smaller than M_P^4 when inflation starts.

The best-fit parameters are obtained by reusing the existing parameters in the publicly available CAMB [13] and COSMOMC codes [14]. Once the initial value for the field, ϵ_1 and the coefficients of the potentials are set, the start of inflation determines the initial scale k that will be used for the mode integration and extrapolation of the primordial spectra for the CAMB code assuming sudden reheating to transfer the scales from GeV to Mpc^{-1} . For each potential a new covariance matrix is found.

When the coefficients m and V_0 in the potentials are varied, this scenario contains one parameter extra than a standard Λ cold dark matter scenario (Λ CDM) with 6 primary parameters. For these cases, the Akaike information criterion and a χ^2 criterion are applied in order to know the goodness of fit for this scenario.

III. RESULTS

The best-fit parameters are calculated for each potential in three cases corresponding to Bunch-Davies initial conditions for the perturbations and kinetic energy domination, varying the coefficients m and V_0 with tensors included and keeping them fixed without tensor modes. To compare with the results found in [2], a simulation for the $\lambda\phi^4$ potential was also performed when the solution for kinetic energy domination is applied to set the initial conditions for the perturbations.

The value of the pivot scale in the Monte Carlo code does not affect the mode integration since the moment when inflation starts with kinetic energy domination determines the initial scale for the integration. Nonetheless, a simulation was done for each potential in order to check that the best-fit parameters were indeed not affected by changing the value of the pivot scale in the COSMOMC code.

In Table I the results of the Monte Carlo simulations are shown for the potentials in Eq. (4); all simulations have been done for 6 chains of 100 000 samples of length each, using WMAP 7-year data including TT, TE and EE spectra only. To account for the number of final independent samples, 20% of rows are excluded from the analysis of the chains. The lensing effect is taken into account in all cases. The values in Table I for the coefficients of the potentials are m/M_P and V_0/M_P^4 respectively.

TABLE I. Results of Monte Carlo integration for kinetic energy domination (k. e. d.) and Bunch–Davies (BD) vacuum initial conditions. The sixth column shows the values for coefficients of the potentials.

	Potential	Initial conditions	$\epsilon_{1,i}$	ϕ_i/M_p	Coefficient	Tensors	independent samples	Burn-in	R-1
1	$\frac{1}{2}m^2\phi^2$	k. e. d.	[2.63, 2.999]	[16.57, 17.97]	$[6.14 \times 10^{-6}, 7.13 \times 10^{-6}]$	included	6985	220	0.0017
2		BD	same	same	same	included	5749	249	0.0028
3		BD	same	same	6.62×10^{-6}	not included	5828	164	0.0021
4	hybrid	k. e. d.	[2.9, 2.999]	[23.6, 24.4]	$[1.73 \times 10^{-10}, 2.12 \times 10^{-10}]$	included	5711	324	0.0022
5		BD	same	same	same	included	3359	212	0.0048

According to the conclusions of [2], the most favored situation for this scenario of inflation corresponds to $\epsilon_{1,i}$ being as close as possible to 3. The results in Table I show the biggest number of final independent samples when the coefficients of both potentials are varied, the tensor modes are included and an initial condition with kinetic energy domination for the perturbations is used. In the case of the hybrid potential, the prior interval of initial values for ϵ_1 that allowed to conclude successfully the simulations had to be reduced to [2.9, 2.999], whereas for the ϕ^2 potential a wider range of initial values for this function is allowed. For all cases a simulation with a pivot scale equal to 0.01 Mpc^{-1} is performed in order to check that the best-fit values are not too different from those with $k_{\text{pivot}} = 0.05 \text{ Mpc}^{-1}$ from the same prior intervals. Only the final number of independent samples depends significantly on the value of the pivot scale. Its value almost doubles for $k_{\text{pivot}} = 0.01 \text{ Mpc}^{-1}$ with respect to 0.05 Mpc^{-1} .

In Table II, the best-fit cosmological parameters are presented when the coefficients of both potentials are varied and tensor modes are included. An initial condition with kinetic energy domination for the perturbations and for Bunch–Davies vacuum shows no differences in the predictions for the parameters. In the case of the hybrid potential, only the results for kinetic energy domination are presented since there are no changes in those values as compared to using Bunch–Davies initial conditions. The same situation applies to the results of the $\lambda\phi^4$ potential when compared to the values for the cosmological parameters found in [2], and therefore the results are omitted here. The distributions of the cosmological parameters for case 1 in Table I are presented in the Appendix. It can be observed that, as in [2], the initial value of the field and $\epsilon_{1,i}$ are degenerate with each other and the only independent parameter for this scenario is the total amount of inflation produced by each model. These two quantities have non Gaussian distributions whereas the distribution for the coefficient of the potential is Gaussian.

As mentioned before, all models with the exception of case 3 presented in Table I, are described by 7 primary parameters, one more than a standard ΛCDM model with 6 parameters. For these cases the Akaike information criterion (AIC) is applied in order to compare the goodness of fit: $\text{AIC} = -2\mathcal{L}_{\text{max}} + 2N_{\text{par}}$ where \mathcal{L}_{max} is the

maximum likelihood of each model and N_{par} is the number of parameters. The results are shown in Table III. The values of ΔAIC for both potentials here are smaller than those for the $\lambda\phi^4$ potential as seen in [2], the difference for the $m^2\phi^2$ potential is the smallest of the three cases. Therefore, the results for these two potentials in this scenario are only marginally worse than the standard ΛCDM scenario.

A. Mode Integration, Spectral index and Running

The results of the mode integration are presented only for the $m^2\phi^2$ potential considering two possibilities : Equations (5), (6), (8) and (9) for the initial conditions of the perturbations. The behavior of the spectral indices $n_{S,T}$, and runnings $\alpha_{S,T}$ for scalar and tensor perturbations using the mode integration is also shown. Two expressions that can be applied when the power spectra are continuous functions are written in the appendix. When they are obtained from a mode integration, they are discrete functions as a result of the integration of Eqs. (1) and (2) for 200 fixed values of the scale k and an alternative way to evaluate the indices and runnings is used. The scales for the mode integration were determined using the first mode, obtained when inflation starts, up to a value five orders of magnitude bigger, spacing the interval into 200 modes.

The results of the mode integration for both power spectra are shown in Fig. 1, they show their behavior for Bunch–Davies vacuum initial conditions, for kinetic energy domination and for slow-roll at first-order. Both initial conditions do not differ significantly from each other when inflation starts. Therefore, as the process of inflation goes on, deeper sub horizon modes coincide with the attractor slow-roll behavior when they are frozen outside the horizon without being affected by different initial conditions even having approximately only 60 e -folds of total accelerated expansion. The oscillations in the numeric solutions appear because, as mentioned in [2], the first modes being integrated are already nearly at the moment of horizon crossing and the oscillatory solutions of the mode equation can be observed.

The behavior of the spectral index and its running for the scalar modes with the expressions written in the ap-

TABLE II. Best-fit cosmological parameters for some of the examples in Table I. The parameter C_P represents the coefficient of the potential divided by M_p and M_p^4 for each potential respectively.

			$\Omega_b h^2$	Ω_{DM}	θ	τ	ϕ_i/M_p	$\epsilon_{1,i}$	$\ln(10^{10} C_P)$	Ω_Λ	Age/Gyr	Ω_m	z_{re}	r_{10}	H_0
$\frac{1}{2}m^2\phi^2$	1,2	μ	0.022	0.11	1.039	0.087	17.47	2.78	11.1	0.73	13.8	0.27	10.48	0.067	70.52
		σ	0.0003	0.005	0.002	0.01	0.3	0.09	0.02	0.03	0.08	0.03	1.2	0.002	1.9
	3	μ	0.023	0.11	1.039	0.09	17.47	2.78	11.1	0.72	13.8	0.28	11.0	-	69.9
		σ	0.0003	0.005	0.002	0.01	0.3	0.09	-	0.02	0.08	0.02	0.7	-	1.6
hybrid	4,5	μ	0.023	0.11	1.041	0.1	24.1	2.93	0.63	0.75	13.6	0.25	11.04	0.03	73.13
		σ	0.0003	0.005	0.002	0.02	0.2	0.02	0.03	0.02	0.1	0.02	1.2	0.001	1.9

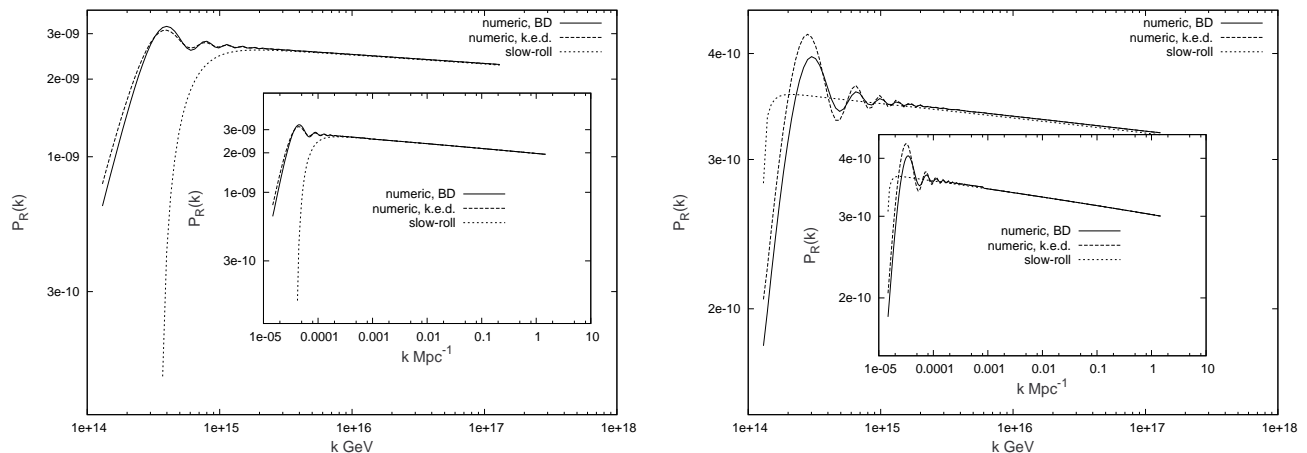


FIG. 1. Mode integration for the scalar and tensor modes from the best-fit value $\epsilon_{1,i} = 2.78$, $\phi_i/M_p = 17.47$, 6.55×10^{-6} with tensors, cases 1 and 2 in Table I.

TABLE III. Akaike information criterion applied to the models presented in Tables I,II with respect to a Λ CDM model of 6 parameters.

Model	$-\ln \mathcal{L}_{\max}$	N_{par}	AIC	Δ AIC	χ^2
Λ CDM	3737.2	6	7486.4	0	7474.4
1	3736.384	7	7486.768	0.368	7472.768
2	3736.39	7	7486.78	0.38	7472.78
4	3737.419	7	7488.838	2.07	7474.838
5	3737.509	7	7489.018	2.25	7475.018

pendix are shown in Fig. 2. In the case of the spectral index, the plot shows the result of the mode integration from the second mode onwards and for the running from the third mode onwards. This is only due to the expression taken to approximate the derivatives of the discrete power spectrum. However, both initial conditions seem to suggest that the initial value of the spectral index is close to or at 3, from which the oscillations of the solutions of the mode equation are also present in the derivatives. A similar behavior is observed for the running. In the case of the spectral index, the derivative is always positive. The behavior of the same quantities for the tensor modes are shown for completeness in the Appendix.

To quantify the predictions of each potential for the best-fit values obtained in the Monte Carlo integration, the slow-roll expressions for the amplitude of the scalar spectrum, the spectral index and the running at first-order in slow-roll are used. They are presented in Table IV for two pivot scales at 0.01, 0.05 Mpc^{-1} , the first three cases of Table I, II give the same predictions since the best-fit values for the initial ϵ_1 and ϕ/M_p are the same. They satisfy the constraint on the amplitude of scalar perturbations at 1 and 2 sigma levels for the analysis of WMAP7 data including running of the spectral index.

B. Low Multipoles

An early epoch of kinetic energy domination has been proposed as an explanation for the smaller than expected power of the low multipoles of the CMB anisotropies [2], [4], [5], [6], [7], [8], [15], [16], [19]. By applying initial conditions for the field, $\epsilon_{1,i}$ and the coefficient of the potential inside the 1σ interval of the best-fit values in Table II, it is possible to find the quadrupole below 200 with values of the tensor-to-scalar ratio, spectral index, running and amplitude of scalar perturbations inside the 1 and 2σ intervals allowed by observations for the analysis with ten-

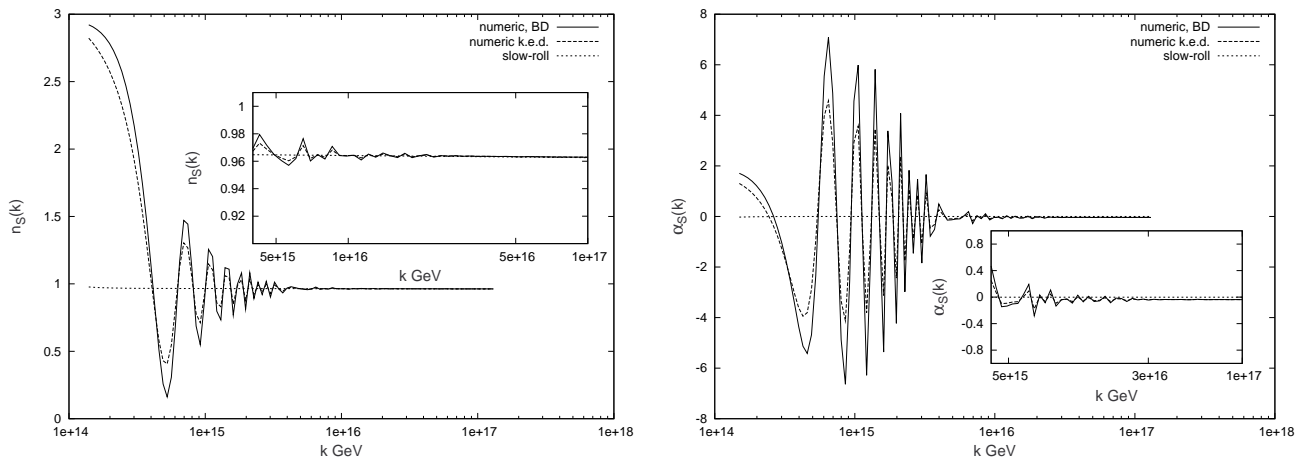


FIG. 2. Behavior of the spectral index and its running for the scalar modes using the mode integration, from the best-fit value $\epsilon_{1,i} = 2.78$, $\phi_i/M_P = 17.47$, 6.55×10^{-6} with tensors, showing cases 1 and 2 in Table I, compared to the slow-roll prediction at first order for the same initial condition.

TABLE IV. Values for inflationary observables at two different pivot scales for the best-fit values presented in Table II, r is the tensor-to-scalar ratio.

	Best-fit values: $\epsilon_{1,i}, \phi_i/M_P, C_P$	N_T	$k_*(Mpc^{-1}), N_*$	r	n_s	$dn_s/dlnk$	Amplitude
1,2,3	2.78, 17.47, $6.55 \times 10^{-6} M_P$	63.2	0.05, 58.3	0.14	0.97	-6.8×10^{-4}	2.45×10^{-9}
			0.01, 59.8	0.13	0.97	-8.99×10^{-3}	2.57×10^{-9}
4,5	2.93, 24.1, $1.88 \times 10^{-10} M_P^4$	61.85	0.05, 56.8	0.056	0.97	-1.7×10^{-4}	2.33×10^{-9}
			0.01, 58.2	0.055	0.99	-6.1×10^{-3}	2.37×10^{-9}

sors and running [3]. However, this happens evaluating these quantities at a scale of $\sim 0.3 Mpc^{-1}$. As the initial conditions give higher values of the quadrupole, the inflationary predictions are met for values of the scale closer to $0.5 Mpc^{-1}$. Some examples of this for each of the potentials in Eq. (4) are provided in Table V. The first and fifth lines show the predictions for the quadrupole using the central values of the best-fit parameters. As for the other examples, one can observe that small changes in the field and $\epsilon_{1,i}$ have a more significant effect than changing the value of the coefficient of the potential. The same is applicable to the results of the hybrid potential.

Although the value for the quadrupole predicted by the best-fit models is not low enough on scales relevant for observations, the suppression of power has more statistical significance for the two-point angular correlation function than for the quadrupole¹ [16], [17]. The two-point correlation function is plotted in Fig. 3 for the central values in Table II, the expression used is:

$$C(\theta) = \frac{1}{4\pi} \sum_{\ell=2}^{\ell_{\max}} (2\ell+1) C_\ell P_\ell(\cos\theta). \quad (11)$$

where C_ℓ is the angular power spectra and P_ℓ Legendre polynomials. The expansion is done for $\ell_{\max} = 30$. For

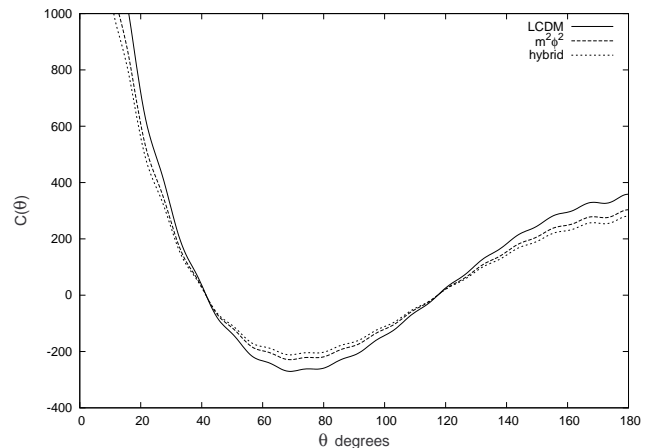


FIG. 3. Two point angular correlation function for the best-fit values of cases 1,2, 4 and 5 in Table II, and a Λ CDM model with $n_s = 0.96$.

angles smaller than approximately 40° , the predictions for this function with the central values of the best-fit models are in general more suppressed than those of the Λ CDM model.

¹ Many thanks to Dominik Schwarz for pointing this out.

TABLE V. Values for the quadrupole and octopole for the best-fit values, of 1, 2, 4 and 5 in Table II.

	ϕ_i/M_P	$\epsilon_{1,i}$	C_P	N_T	Quadrupole	Octopole	r	n_s	$dn_s/d \ln k$	Amplitude	N_*	$k_*(\text{Mpc}^{-1})$	
$m^2\phi^2$	1	17.47	2.78	$6.55 \times 10^{-6} M_P$	63.2	1120.6	1050.0	0.14	0.97	-6.8×10^{-4}	2.45×10^{-9}	58.3	0.05
	2	16.94	2.78	$6.57 \times 10^{-6} M_P$	59.1	194.94	209.04	0.14	0.99	-0.066	2.27×10^{-9}	56.35	0.35
	3	17.3	2.85	$6.56 \times 10^{-6} M_P$	60.52	656.62	717.42	0.14	0.99	-0.08	2.36×10^{-9}	57.9	0.08
	4	17.35	2.85	$6.56 \times 10^{-6} M_P$	60.9	820.91	919.51	0.14	0.99	-0.06	2.4×10^{-9}	58.2	0.057
hybrid	5	24.1	2.93	$1.88 \times 10^{-10} M_P^4$	61.85	1035.9	973.25	0.056	0.99	-2×10^{-4}	2.33×10^{-9}	56.79	0.053
	6	23.9	2.95	$1.88 \times 10^{-10} M_P^4$	57.71	213.42	220.11	0.057	1.0	-0.041	2.23×10^{-9}	54.7	0.42
	7	24.0	2.94	$1.88 \times 10^{-10} M_P^4$	59.86	942.37	995.96	0.056	1.0	-0.037	2.3×10^{-9}	56.8	0.052
	8	23.95	2.94	$1.83 \times 10^{-10} M_P^4$	59.25	683.31	753.49	0.056	0.99	-0.037	2.22×10^{-9}	56.2	0.094

IV. DISCUSSION

The implementation of the $m^2\phi^2$ and hybrid potentials for an early stage of kinetic energy domination with only the sufficient amount of accelerated expansion gives results consistent with those found before for the $\lambda\phi^4$ potential. The distributions of the quantities that set the initial conditions for this scenario, that is the initial values of the scalar field and the function ϵ_1 , show a degeneracy between each other, which confirms that the only independent parameter for this scenario is the total amount of inflation produced. The mode integration for these potentials shows again the presence of a cutoff of power on large scales. The spectral indices and the runnings obtained from the mode integration show the oscillations of the solutions of the mode equations of perturbations before the system joins the inflationary slow-roll attractor. In accordance with the results of [2], initial conditions inside the 1σ interval of the best-fit values for the field and ϵ_1 can give a significant suppression of power on the largest scales, and reproduce the value of the quadrupole at very large scales. At $k_* = 0.05 \text{Mpc}^{-1}$ there is already a suppression of power but not large enough to be consistent with observations. Additionally, the behavior of the two-point angular correlation function shows that on large angular scales, the power is suppressed for the best-fit models of the $m^2\phi^2$ and hybrid potentials with respect to the ΛCDM case.

As mentioned before, the pivot scale set to do the Monte Carlo integration must not alter the results for the best-fit parameters as was found here by running a simulation for the same intervals with a different value of this quantity (0.01Mpc^{-1}). What did change was the final number of independent samples, which in some cases is almost twice the amount of them as compared to a pivot scale of 0.05Mpc^{-1} . Whether this has a physical significance is not further investigated here.

Another aspect of this work is the use of initial conditions for the perturbations consistent with an early stage of kinetic energy domination. The results of the mode integration show no significant alteration with respect to the usual initial conditions in the vacuum, the solutions rapidly join the slow-roll attractor and they have in fact a less sharp cutoff of power on large scales. This how-

ever, does not affect the values of the best-fit parameters obtained from the same prior intervals for Bunch–Davies vacuum initial conditions and a homogeneous initial condition in kinetic energy domination.

Another point to mention is, that similarly to the results for the $\lambda\phi^4$ potential, the biggest number of final independent samples was found for those initial conditions with $\epsilon_{1,i} \simeq 3$. This perhaps can again be interpreted as an indication that this initial condition represents the most favored situation for this scenario.

Since the use of initial conditions for the perturbations different from the vacuum does not alter the predictions of this scenario, an interesting possibility for further exploration would be its application to multi field inflation scenarios. For these cases, perhaps the effect of the suppression of power on large scales could have a more significant influence on the predictions of this scenario.

V. ACKNOWLEDGMENTS

This research was supported by the DFG cluster of excellence "Origin and Structure of the Universe". It is a pleasure to thank Dominik Schwarz, Houri Ziaee-pour and Christoph R ath for comments and revision of the manuscript. I thank Sandipan Kundu for interesting comments and discussion and H. J. de Vega and S ebastien Clesse for hints to the literature. I acknowledge the use of the Linux Cluster of the Leibniz-Rechenzentrum der Bayerischen Akademie der Wissenschaften. The use of the CAMB and COSMOMC packages as well as WMAP 7-yr data from the LAMBDA server are also acknowledged.

Appendix A: Spectral indices and runnings

Applying the definition of the spectral indices and their runnings, as given for example in [11]:

$$n_S(k) - 1 \equiv \frac{d \ln P_R}{d \ln k}, \quad n_T \equiv (k) \frac{d \ln P_T}{d \ln k}, \quad (\text{A.1})$$

$$\alpha_S(k) \equiv \frac{dn_S}{d \ln k}, \quad \alpha_T(k) \equiv \frac{dn_T}{d \ln k},$$

where P_S and P_T are given by Eq. (10), one arrives to the following expressions for the spectral indices:

$$n_S - 1 = \frac{1}{(1 - \epsilon_1)} \left[1 - 3\epsilon_1 - \epsilon_2 + 2 \frac{d \ln |u_k^S|}{dN} \right] \quad (\text{A.2})$$

$$n_T = \frac{1}{(1 - \epsilon_1)} \left[1 - 3\epsilon_1 + 2 \frac{d \ln |u_k^T|}{dN} \right]$$

and for the runnings :

$$\alpha_S = \frac{1}{(1 - \epsilon_1)^2} \left[2 \frac{d^2 \ln |u_k^S|}{dN^2} - \epsilon_2(3\epsilon_1 + \epsilon_3) + \epsilon_1 \epsilon_2 (n_S - 1) \right] \quad (\text{A.3})$$

$$\alpha_T = \frac{1}{(1 - \epsilon_1)^2} \left[2 \frac{d^2 \ln |u_k^T|}{dN^2} + \epsilon_1 \epsilon_2 (n_T - 3) \right]$$

evaluated at $k = aH$, the moment of horizon crossing for each perturbation mode. If one substitutes the expressions of $u_k^{S,T}$ using the Stewart–Lyth solutions for the mode equations [18]:

$$|u_k^S| \simeq \frac{1}{\sqrt{aH}} \left[1 - \epsilon_1(1 + C) - \frac{C}{2} \epsilon_2 \right], \quad (\text{A.4})$$

$$|u_k^T| \simeq \frac{1}{\sqrt{2aH}} [1 - (1 + C)\epsilon_1],$$

where $C = -2 + \ln 2 + \gamma \simeq -0.73$, one recovers the usual slow-roll expressions at first-order:

$$n_S \simeq 1 - 2\epsilon_1 - \epsilon_2, \quad \alpha_S \simeq -\epsilon_2(2\epsilon_1 + \epsilon_3), \quad (\text{A.5})$$

$$n_T \simeq -2\epsilon_1, \quad \alpha_T \simeq -2\epsilon_1 \epsilon_2.$$

From the mode integration one obtains the values for the amplitudes of the spectra for a series of values of the modes k . They are therefore discrete functions and the previous expressions if applied, do not give as expected a result that should join the slow-roll attractor given by Equations (A.5). One therefore needs to evaluate the derivative of the spectra as a discrete function directly. In this case, the backwards difference approximation for the first and second derivatives of the power spectra are used. For an arbitrary function $P(k_i)$:

$$\frac{dP(k_i)}{dk_i} \simeq \frac{P(k_{i+1}) - P(k_i)}{k_{i+1} - k_i}, \quad (\text{A.6})$$

$$\frac{d^2 P(k_i)}{dk_i^2} \simeq \frac{P(k_{i+2}) - 2P(k_{i+1}) + P(k_i)}{(k_i - k_{i-1})^2}$$

after substituting in Equations (A.1):

$$n_S = 1 + \frac{k}{P_R} \frac{dP_R}{dk}, \quad n_T = \frac{k}{P_T} \frac{dP_T}{dk} \quad (\text{A.7})$$

$$\alpha_{S,T} = k \frac{dn_{S,T}}{dk} = \frac{k^2}{P_{R,T}} \frac{d^2 P_{R,T}}{dk^2} + \frac{k}{P_{R,T}} \frac{dP_{R,T}}{dk} - \left(\frac{k}{P_{R,T}} \frac{dP_{R,T}}{dk} \right)^2.$$

In this case, the spectral indices are evaluated from the second mode onwards and the runnings from the third onwards. The behavior of the spectral index and its running for the tensor modes are shown in Fig. 4. The distributions of cosmological parameters for case 1 in Table I are presented in Fig. 5

-
- [1] A. D. Linde, “Chaotic Inflation,” *Phys. Lett. B* **129** (1983) 177.
- [2] E. Ramirez and D. J. Schwarz, “Predictions of just-enough inflation,” arXiv:1111.7131 [astro-ph.CO]. D. J. Schwarz and E. Ramirez, “Just enough inflation,” arXiv:0912.4348 [hep-ph]. E. Ramirez and D. J. Schwarz, “ ϕ^4 inflation is not excluded,” *Phys. Rev. D* **80**, 023525 (2009) [arXiv:0903.3543 [astro-ph.CO]].
- [3] E. Komatsu *et al.* [WMAP Collaboration], “Seven-Year Wilkinson Microwave Anisotropy Probe (WMAP) Observations: Cosmological Interpretation,” *Astrophys. J. Suppl.* **192**, 18 (2011) [arXiv:1001.4538 [astro-ph.CO]].
- [4] C. R. Contaldi, M. Peloso, L. Kofman and A. Linde, “Suppressing the lower Multipoles in the CMB Anisotropies,” *JCAP* **0307**, 002 (2003) [arXiv:astro-ph/0303636].
- [5] D. Boyanovsky, H. J. de Vega and N. G. Sanchez, “CMB quadrupole suppression. 2. The early fast roll stage,” *Phys. Rev. D* **74**, 123007 (2006) [astro-ph/0607487]; C. Destri, H. J. de Vega and N. G. Sanchez, “The CMB Quadrupole depression produced by early fast-roll inflation: MCMC analysis of WMAP and SDSS data,” *Phys. Rev. D* **78**, 023013 (2008) [arXiv:0804.2387 [astro-ph]]; F. J. Cao, H. J. de Vega and N. G. Sanchez, “Quantum slow-roll and quantum fast-roll inflationary initial conditions: CMB quadrupole suppression and further effects on the low CMB multipoles,” *Phys. Rev. D* **78**, 083508 (2008) [arXiv:0809.0623 [astro-ph]]; C. Destri, H. J. de Vega and N. G. Sanchez, “The pre-inflationary and inflationary fast-roll eras and their signatures in the low CMB multipoles,” *Phys. Rev. D* **81**, 063520 (2010) [arXiv:0912.2994 [astro-ph.CO]].
- [6] J. F. Donoghue, K. Dutta and A. Ross, “Non-isotropy in the CMB power spectrum in single field inflation,” *Phys. Rev. D* **80**, 023526 (2009) [astro-ph/0703455 [ASTRO-PH]].
- [7] B. A. Powell and W. H. Kinney, “The pre-inflationary vacuum in the cosmic microwave background,” *Phys. Rev. D* **76**, 063512 (2007) [astro-ph/0612006].
- [8] I. C. Wang and K. W. Ng, “Effects of a pre-inflation radiation-dominated epoch to CMB anisotropy,” *Phys. Rev. D* **77**, 083501 (2008) [arXiv:0704.2095 [astro-ph]].
- [9] V. F. Mukhanov, H. A. Feldman and R. H. Brandenberger, “Theory of cosmological perturbations. Part 1. Classical perturbations. Part 2. Quantum theory of perturbations. Part 3. Extensions,” *Phys. Rept.* **215**, 203 (1992).
- [10] D. J. Schwarz, C. A. Terrero-Escalante and A. A. Garcia, “Higher order corrections to primordial spectra from cosmological inflation,” *Phys. Lett. B* **517**, 243 (2001) [arXiv:astro-ph/0106020].
- [11] S. M. Leach, A. R. Liddle, J. Martin and D. J. Schwarz, “Cosmological parameter estimation and the inflationary cosmology,” *Phys. Rev. D* **66**, 023515 (2002)

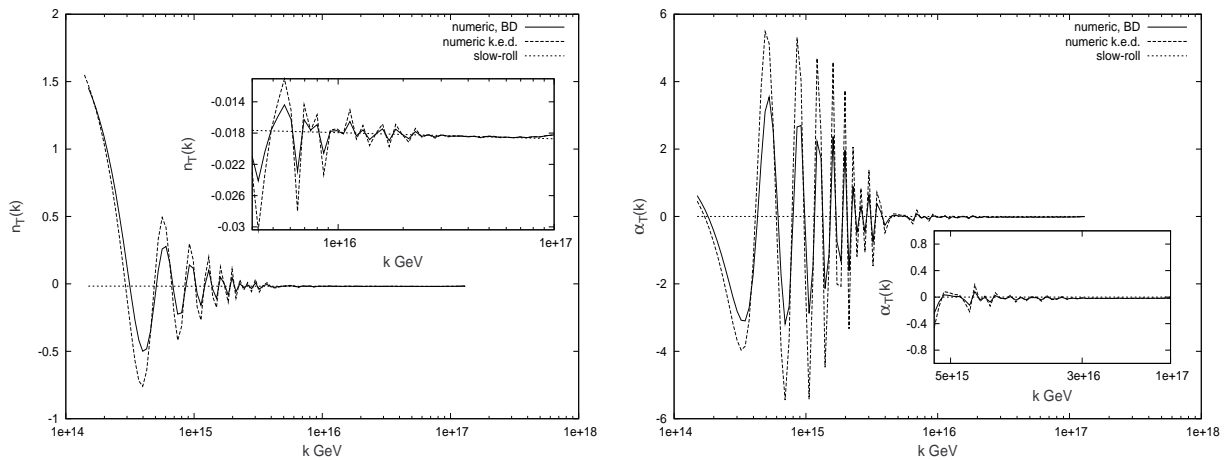


FIG. 4. Behavior of the spectral index and its running for the tensor modes using the mode integration, from the best-fit value $\epsilon_{1,i} = 2.78$, $\phi_i/M_p = 17.47$, 6.55×10^{-6} with tensors, cases 1 and 2 in Table I, compared to the slow-roll prediction at first order for the same initial condition.

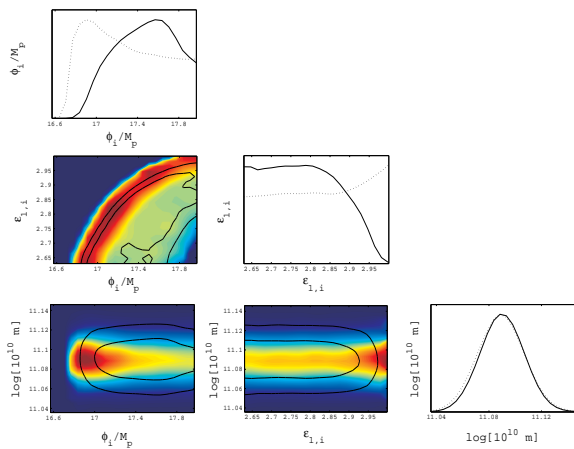


FIG. 5. (color online). Three dimensional distributions of cosmological parameters for cases 1 and 2 in Table II.

[arXiv:astro-ph/0202094].

- [12] S. Clesse, “Hybrid inflation along waterfall trajectories,” *Phys. Rev. D* **83**, 063518 (2011) [arXiv:1006.4522 [gr-qc]].
- [13] A. Lewis, A. Challinor and A. Lasenby, “Efficient computation of CMB anisotropies in closed FRW models,” *Astrophys. J.* **538**, 473 (2000) [astro-ph/9911177].
- [14] A. Lewis and S. Bridle, “Cosmological parameters from CMB and other data: A Monte Carlo approach,” *Phys.*

Rev. D **66**, 103511 (2002) [arXiv:astro-ph/0205436].

- [15] C. J. Copi, D. Huterer, D. J. Schwarz and G. D. Starkman, “No large-angle correlations on the non-Galactic microwave sky,” arXiv:0808.3767 [astro-ph].
- [16] D. J. Schwarz, G. D. Starkman, D. Huterer and C. J. Copi, “Is the low- l microwave background cosmic?,” *Phys. Rev. Lett.* **93**, 221301 (2004) [arXiv:astro-ph/0403353]; C. Copi, D. Huterer, D. Schwarz and G. Starkman, “The Uncorrelated Universe: Statistical Anisotropy and the Vanishing Angular Correlation Function in WMAP Years 1-3,” *Phys. Rev. D* **75**, 023507 (2007) [arXiv:astro-ph/0605135].
- [17] D. Sarkar, D. Huterer, C. J. Copi, G. D. Starkman and D. J. Schwarz, “Missing Power vs low- l Alignments in the Cosmic Microwave Background: No Correlation in the Standard Cosmological Model,” *Astropart. Phys.* **34**, 591 (2011) [arXiv:1004.3784 [astro-ph.CO]].
- [18] E. D. Stewart and D. H. Lyth, “A more accurate analytic calculation of the spectrum of cosmological perturbations produced during inflation,” *Phys. Lett. B* **302**, 171 (1993) [gr-qc/9302019].
- [19] G. Hinshaw *et al.*, “2-Point Correlations in the COBE DMR 4-Year Anisotropy Maps,” *Astrophys. J.* **464**, L25 (1996) arXiv:astro-ph/9601061; D. N. Spergel *et al.* [WMAP Collaboration], “First Year Wilkinson Microwave Anisotropy Probe (WMAP) Observations: Determination of Cosmological Parameters,” *Astrophys. J. Suppl.* **148**, 175 (2003) [arXiv:astro-ph/0302209].